Long-term effects of chronic nicotine exposure on brain nicotinic receptors

Morgane Besson[†], Sylvie Granon[†‡], Monica Mameli-Engvall[§], Isabelle Cloëz-Tayarani[†], Nicolas Maubourguet[†], Anne Cormier[†], Pierre Cazala[¶], Vincent David[¶], Jean-Pierre Changeux[†‡], and Philippe Faure[†‡]

[†]''Récepteurs et Cognition,'' Centre National de la Recherche Scientifique Unité de Recherche Associée 2182, ''Unité de Neurobiologie Intégrative des Systémes Cholinergiques,'' Institut Pasteur, 75724 Paris, France; [§]Department of Physiology and Pharmacology, Karolinska Institute, S-171 77 Stockholm, Sweden; [¶]Centre National de la Recherche Scientifique Unité Mixte de Recherche 5106, Neurosciences Cognitives, Université Bordeaux 1, 33405 Talence, France

Contributed by Jean-Pierre Changeux, March 27, 2007 (sent for review March 2, 2007)

Chronic nicotine exposure results in long-term homeostatic regulation of nicotinic acetylcholine receptors (nAChRs) that play a key role in the adaptative cellular processes leading to addiction. However, the relative contribution of the different nAChR subunits in this process is unclear. Using genetically modified mice and pharmacological manipulations, we provide behavioral, electrophysiological, and pharmacological evidence for a long-term mechanism by which chronic nicotine triggers opposing processes differentially mediated by β2*- vs. α7*nAChRs. These data offer previously undescribed insights into the understanding of nicotine addiction and the treatment of several human pathologies by nicotine-like agents chronically acting on β2*- or α7*nAChRs.

exploratory behaviors | homeostatis | ventral tegmental area | opponent process

Nicotine is the main active substance of tobacco that causes addiction by altering reward systems and relevant psychomotor and cognitive processes via its specific action on nicotinic acetylcholine receptors (nAChRs) (1). Acute injection of nicotine increases the firing rates and bursting patterns of dopamine (DA) neurons in the ventral tegmental area (VTA) (2), enhances DA release in the nucleus accumbens (3), and modifies locomotor activity (4). Furthermore, systemic or intra-VTA injection of nicotine elicits self-administration (5–9) and conditioned place preference (10). These effects disappear in mice lacking high-affinity β2-subunit containing nAChRs (β2*nAChRs) (7, 9, 11) and are restored by reexpression of the β2-subunit in VTA neurons (8).

However, and although this also may be a function of the behavior measured and the species and doses used, repeated or chronic exposure to nicotine may not cause any apparent changes of behavior until the organism is deprived of the drug. Cessation of nicotine delivery then produces a withdrawal syndrome that reveals latent modifications of brain circuits consequent to chronic nicotine exposure (12). It has been suggested that nAChRs desensitization and subsequent up-regulation might be involved in these long-term effects of nicotine (13–15). However, recent evidence (16, 17) suggests that both β2*nAChRs and non-β2*nAChRs, most likely α7*nAChRs, are involved in these chronic nicotine effects, even though α7*nAChRs do not up-regulate (16). Furthermore, most of the studies reporting adaptations in nAChRs under chronic nicotine have been conducted *in vitro*, and knowledge regarding modifications caused by nicotine *in vivo* appears as essential for the understanding of the mechanisms of withdrawal and tolerance.

Yet the neural mechanisms mediating the long-term effects of nicotine *in vivo*, in particular the subtypes of nicotinic receptors concerned, remain largely unknown. In the present study, using a mouse model, we address the issue of the modifications caused by chronic nicotine exposure and the differential contribution of the various nAChRs subtypes in behavioral (exploratory behaviors) and electrophysiological (VTA DA neurons firing patterns) paradigms that are known to be specifically modified by an alteration of the β2*nAChRs (8, 11, 18). Furthermore, in contrast to other studies that focus on withdrawal, i.e., after cessation of nicotine administration (15, 19, 20), we describe here *in vivo* modification under chronic nicotine. In our experiments, the dose of nicotine used was selected to maintain a plasma concentration of nicotine analogous to that observed in smokers (21), which was shown to be sufficient to cause a withdrawal syndrome in wild-type (WT) mice (7).

Our study demonstrates that long-term nicotine exposure under our experimental conditions does not cause any apparent effects in WT mice, neither at the behavioral nor at the DA electrophysiological levels, even though nicotine exposure elicits the expected up-regulation of β2*nAChRs. It further shows that in WT mice, β2*and α7*-nAChRs differentially contribute to long-lasting processes that maintain homeostasis as long as nicotine is available. Indeed (*i*) chronic nicotine treatment, through its action on α7*nAChRs, largely restores the behavioral and electrophysiological deficits previously associated with the lack of β2*nAChRs in mice; and (*ii*) WT mice under chronic nicotine display a phenotype analogous to that of β2-KO mice when α7*nAChRs are pharmacologically blocked. We here propose that the coordinated processes that act through both receptors subtypes and that ultimately maintain homeostasis represent some of the long-term changes at the origin of nicotine addiction.

Results

Chronic exposure to nicotine is known, in both humans and rats, to cause an up-regulation of nAChRs, especially of heteromeric receptors, most likely non-α7*nAChRs (22–24). We confirm here, in WT mice, that long-term exposure to nicotine elicits up-regulation of β2*nAChRs. Quantitative receptor autoradiography (see *Methods*) using [^{125}I]-epibatidine and [^{125}I]α-bungarotoxin as ligands labeling, respectively, the high- and low-affinity nAChR binding sites, showed significant increases in high-affinity binding in lateral septum, caudate putamen, and nucleus accumbens after chronic treatment (Fig. 1*A*), whereas the densities of low-affinity nicotinic binding sites were not affected [see supporting information (SI) Fig. 6].

Author contributions: M.B. and S.G. contributed equally to this work; M.B., S.G., J.-P.C., and P.F. designed research; M.B., S.G., M.M.-E., I.C.-T., N.M., A.C., P.C., and V.D. performed research; M.B., I.C.-T., and P.F. analyzed data; and M.B., S.G., I.C.-T., J.-P.C., and P.F. wrote the paper.

The authors declare no conflict of interest.

Freely available online through the PNAS open access option.

Abbreviations: nAChR, nicotinic acetylcholine receptor; β2*nAChR, β2-subunit containing nAChR; CA, activity in the central zone; CI, inactivity in the central zone; DA, dopamine; MLA, methyllycaconitine; PA, activity in the peripheral zone; VTA, ventral tegmental area.

[‡]To whom correspondence may be addressed. E-mail: granon@pasteur.fr, changeux@pasteur.fr, and phfaure@pasteur.fr.

This article contains supporting information online at www.pnas.org/cgi/content/full/0702698104/DC1.

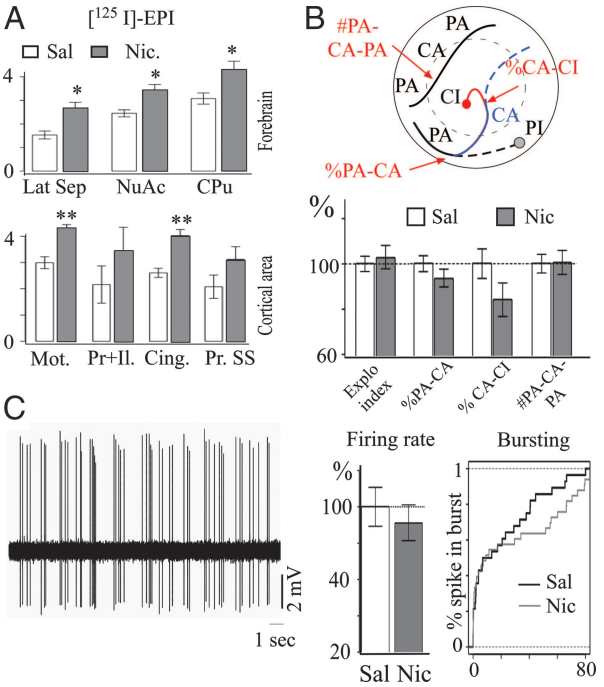

Fig. 1. Effect of chronic nicotine on WT mice. (*A*) Semiquantitative analysis indicates that [125I]-epibatidine binding increases under chronic nicotine treatment in regions such as LatSep, NuAc, CPu, Mot., Pr+Il., Cing., and Pr. SS. Results are expressed in arbitrary units (mean ± SEM, $n = 4–6$ animals per group; two samples Wilcoxon test, *, $P < 0.05$; **, $P < 0.01$). LatSep, lateral septum; NuAc, nucleus accumbens; CPu, caudate putamen; Pr. SS, primary somatosensory cortex; Pr+Il, prelimbic and infralimbic cortex; Cing, cingulate cortex; Mot., motor cortex. (*B*) Effect of chronic nicotine on WT mice behavior. (*Upper*) Open-field experimental analysis. Four parameters quantifying exploratory behaviors in open-field were used (see *Methods*). The index of exploration defined as the ratio of the time spent in exploration divided by time spent in navigation. %PA-CA, the conditional probability of transition from state PA to state. %CA-CI, the conditional probability of transition from state CA to state CI. (#PA-CA-PA, the total number of large movements across the center of the open-field sequences. (*Lower*) Comparison of parameters quantifying exploratory behaviors in saline condition ($n = 29$) and under nicotine exposure ($n = 34$). These parameters are normalized by values obtained in WT animal under saline condition (=100%, horizontal dashed line). Detailed analyses of behavior indicate no effect of nicotine on the time spent in navigation over the time spent in exploration (Explo index), % PA-CA, % CA-CI, or #PA-CA-PA. Two samples Student's *t* test, df = 61; $P = 0.62$, 1, 0.24, and 0.12, respectively. (*C*) Effect of chronic nicotine on VTA DA neuron firing pattern of WT mice. (*Left*) Sample raw traces of DA neuron firing patterns. (*Right*) Firing pattern analysis after Sal (WT sal, $n = 28$) or Nic exposure (WT nic, $n = 33$). Barplot of mean frequency of VTA DA neurons (two samples Student's *t* test, df = 59; $P = 0.55$). Cumulative distribution of percentage of burst firing (Wilcoxon test; $P = 0.62$).

In an attempt to ascertain whether the observed up-regulation of β2*nAChRs is associated with behavioral effects, we investigated the exploratory behavior of WT mice under conditions of long-term nicotine exposure. As reported in previous investigations (see *Methods* for details), mice exposed to a novel open-field environment display several types of displacements, some of them being affected by the deletion of the β2-subunit gene (18). It then was expected that chronic nicotine, by acting on β2*nAChRs in WT mice, may cause a modification of open-field behaviors. The spatiotemporal sequential organization of exploratory behavior of mice can be evaluated quantitatively by the analysis of the following four parameters (Fig. 1*B* and see *Methods*): (*i*) the time spent in navigation over the time spent in exploration, (*ii*) the probability of a fast peripheral trajectory to be followed by a fast center movement, (*iii*) the probability of a fast center movement to be followed by a pause in the center, and (*iv*) the number of fast crossings through the center. WT mice chronically exposed to nicotine did not show any significant alteration of any of these four parameters as compared with untreated animals (Fig. 1*B*).

We then turned to electrophysiological analysis of VTA DA cell firing. Long-term exposure to nicotine has been reported to modify the synaptic properties of the afferent projections to VTA DA neurons *in vitro* (25). Also, we previously showed that acute exposure to nicotine increases the activity of VTA DA neurons in WT mice (11). Yet, no information regarding long-term modifications of the firing pattern of VTA DA neurons during chronic exposure is available from *in vivo* studies. Thus, extracellular single-unit recordings (Fig. 1*C Left*) were obtained from VTA DA neurons in anesthetized mice under either saline or chronic nicotine administration. All of the recorded neurons fulfilled the three criteria used to identify VTA DA neurons (11, 26). We observed that in animals chronically exposed to nicotine, the distribution of firing rate (Fig. 1*C Center*) and the percentage of spikes (%SWB) within a burst (Fig. 1*C Right*) did not show any detectable modification (see *Methods* for burst identification).

A possible interpretation for the absence of any apparent effects of chronic nicotine on exploratory behavior or on electrophysiological activity of VTA DA neurons, is that, in the WT mouse, long-term changes are revealed only upon the cessation of nicotine delivery and, in fact, are masked during the presence of nicotine. To unravel the underlying processes, we developed a strategy based on the analysis of knockout mice deleted for the β2-subunit. These $\beta2^{-/-}$ mice were shown to display (*i*) a normal withdrawal syndrome after cessation of nicotine delivery (7, 27), suggesting that these animals maintain a form of sensitivity to nicotine, most likely via non-β2*nAChRs receptors and (*ii*) an impairment of VTA DA neuronal activity and exploratory behavior (11, 18), two phenotypes that have been directly linked to the absence of β2*nAChRs in the VTA (8) and for which the possibility of a developmental compensation is unlikely.

Unexpectedly, in $\beta2^{-/-}$ mice, chronic exposure to nicotine significantly altered all four exploratory parameters described above. As illustrated in Fig. 2*A*, two parameters (fast crossing through the center, i.e., PA-CA-PA and the frequency of stops at the center, i.e., %CA-CI) were fully restored up to WT level and two were brought to an intermediate level in between WT and $\beta2^{-/-}$ mice. Therefore, despite the absence of β2*nAChRs, long-term nicotine treatment significantly compensated the exploratory deficit observed in $\beta2^{-/-}$ mice. To elucidate, whether this nicotine-elicited compensation was due to the current ongoing delivery of the drug or to long-term changes elicited by nicotine, a control short-term (3 days) exposure to nicotine was tested and was shown to have little, if any, effect on exploratory behavior, therefore revealing the need for more long-term exposure to nicotine (see *SI Text* and Fig. 7). At the electrophysiological level, chronic nicotine treatment elicited a slight, although nonsignificant, increase in firing rate (Fig. 2*B*), but a major increase in bursting (Fig. 2*C*). As a result, DA neuronal firing patterns of $\beta2^{-/-}$ mice receiving nicotine no longer differed from those exhibited by WT mice.

We then attempted to unravel the mechanisms responsible for these compensatory processes. In $\beta2^{-/-}$ mice submitted to chronic nicotine treatment, neither up-regulation of the persisting heteromeric non-β2 receptors nor of the homomeric nAChRs sites were observed (see SI Fig. 6). Compensatory effects of nicotine cannot be related to increased levels of persisting heteromeric non-β2 receptors and homomeric receptors. However, this does not exclude the existence of other nAChR alterations leading to receptor dysfunction. On the other hand, it was proposed that, in the $\beta2^{-/-}$ mice, the observed changes of exploratory activity and of DA firing and bursting

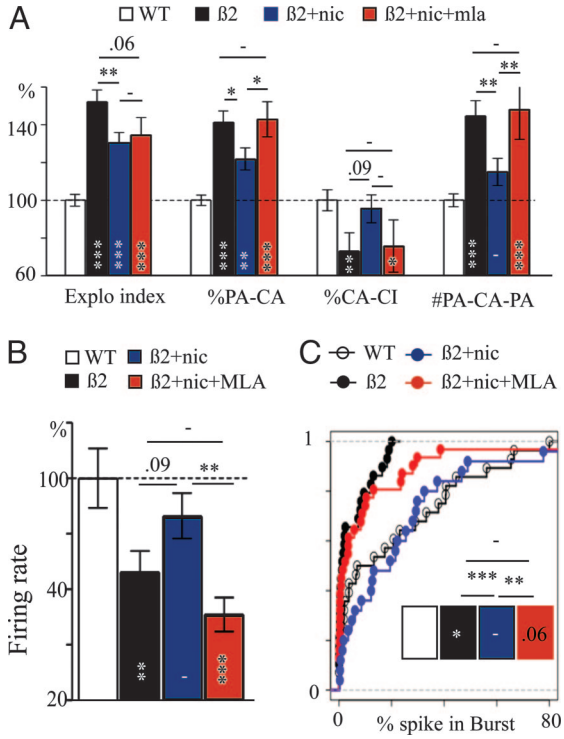

Fig. 2. Restoration by chronic nicotine in $\beta2^{-/-}$ mice is blocked by MLA. (*A*) Comparison of parameters quantifying exploratory behaviors in saline condition ($n = 15$), under nicotine exposure ($n = 19$) and nicotine + MLA exposure ($n = 10$) in $\beta2^{-/-}$ mice. These parameters are normalized (=100%; horizontal dashed line, mean ± SEM) by values obtained in WT animal under saline condition ($n = 29$). We first confirmed our previous results (18) showing that exploratory behavior was different between WT and $\beta2^{-/-}$ mice for the four behavioral parameters we chose. ANOVA indicate statistically significant differences between the four groups $F(3, 69) = 6e\text{-}10$, $2e\text{-}10$, 0.01, and $1.4e\text{-}5$ for the four parameters, respectively. Probabilities of post hoc comparisons between two means are indicated above corresponding horizontal lines except for comparisons with WT that are indicated within the vertical bar. (*B* and *C*) Firing pattern analysis in WT under saline condition ($n = 28$ cells) and in $\beta2^{-/-}$ under saline condition ($n = 29$ neurons), under nicotine exposure ($n = 25$ neurons), and nicotine + MLA exposure ($n = 31$ neurons). (*B*) Barplot of mean frequency of VTA DA neurons (mean ± SEM) normalized (=100%; horizontal dashed line) to the frequency observed in WT animals. ANOVA indicate statistically significant differences between the four groups $F(3, 109) = 2e\text{-}4$. Probability of post hoc comparisons between two means are indicated above corresponding horizontal lines except for comparisons with WT that are indicated within the vertical bar. (*C*) Cumulative distribution of percentage of burst firing. Kruskal–Wallis rank sum test, $P = 0.0007$. Probability of post hoc comparisons (Wilcoxon test) between two means are indicated above corresponding horizontal lines except for comparisons with WT that are indicated within the box. (−, $P > 0.05$; *, $P < 0.05$; **, $P < 0.01$; ***, $P < 0.001$)

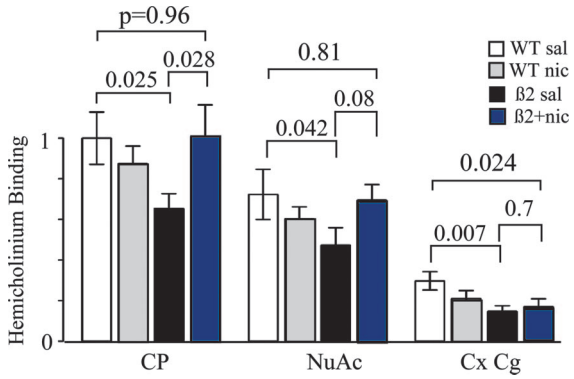

Fig. 3. Level of [^{3}H]-hemicholinium-3 binding is restored by chronic nicotine in $\beta2^{-/-}$ mice. In $\beta2^{-/-}$ mice, [^{3}H]-hemicholinium-3 binding is decreased under control conditions as compared with WT mice in CP, NuAc and Cx Cg regions. Under chronic nicotine, densities of binding are restored in $\beta2^{-/-}$ mice in caudate putamen but not in Cg-Cx, and partially restored in NuAc (mean ± SEM, 6–8 animals per group, *P* values are indicated). CP, caudate putamen; CxCg, cingulate cortex.

resulted from the missing effect of endogenously released acetylcholine on $\beta2$*nAChRs (8, 11). An alteration of the level of tonic cholinergic transmission after chronic nicotine treatment thus was hypothesized. [^{3}H]Hemicholinium-3 was used as a selective ligand to label and quantify the density of high-affinity choline uptake sites, a measure proposed to be a relevant index of the level of cholinergic activity *in vivo* (28). As already shown (29), high-affinity choline uptake sites were detected predominantly in the caudate putamen, nucleus accumbens, and cingulate cortex. We observed that, in the absence of nicotine treatment, levels of bound hemicholinium differed between WT and $\beta2^{-/-}$ mice in caudate putamen, nucleus accumbens, and cingulate cortex (Fig. 3). Finally, we showed that chronic nicotine treatment in $\beta2^{-/-}$ mice led to the recovery of a normal number of choline uptake sites in the caudate putamen and tended to increase it in the nucleus accumbens, but had no effect in the cingulate cortex. On the other hand, no detectable effects were observed in nicotine-treated WT mice in any of the regions of interest (Fig. 3).

It remains unknown which subtype of nicotinic receptors mediates the effects of chronic nicotine observed on open-field behavioral activity, DA neurons, or the activity of striatal cholinergic neurons. A plausible candidate was $\alpha7$*nAChRs, which are the most common subunit in $\beta2^{-/-}$ mice. We therefore tested whether the inhibition of $\alpha7$*nAChRs in $\beta2^{-/-}$ mice receiving nicotine would block the previously established restorative effect of nicotine. For that purpose, $\beta2^{-/-}$ mice were chronically exposed to methyllycaconitine (MLA), an $\alpha7$*nAChRs antagonist, in combination with long-term delivery of nicotine. We observed that, under these conditions, MLA antagonized the restorative effect of nicotine on three of the four behavioral parameters: (*i*) the probability of fast moves from the periphery to the center, (*ii*) the probability of slowing down in the center, and (*iii*) the probability of fast crossing through the center (Fig. 2*A*). MLA also abolished the restorative effects on firing rate (Fig. 2*B*) and bursting (Fig. 2*C*), yielding activity levels statistically similar to those measured in $\beta2^{-/-}$ mice under saline condition. Electrophysiological modifications observed in the firing pattern of VTA DA neurons again correlated well with those observed at the behavioral level.

These data reveal that the restorative effects caused by chronic nicotine in $\beta2^{-/-}$ mice are associated with a long-term plasticity of the cholinergic system that involves $\alpha7$*nAChRs. We then wondered whether such plasticity of the cholinergic system would occur in WT animals, despite the apparent lack of effects of long-term nicotine exposure. WT mice thus were chronically exposed to the nicotine + MLA combination. Behavioral results showed that two of the four exploratory parameters were significantly altered. The behavior of the WT mice became undistinguishable from that of $\beta2^{-/-}$ mice (Fig. 4*A*). To ascertain that MLA blocked a process triggered by chronic nicotine and did not produce any effect by itself, we treated WT mice with MLA alone. We observed that MLA did not alter any of the behavioral parameters measured (See *SI Text* and Fig. 7). Finally, WT mice exposed to the nicotine + MLA combination displayed electrophysiological parameters (Fig. 4 *B* and *C*) at intermediate levels between those measured in $\beta2^{-/-}$ mice ($P = 0.15$ and $P = 0.13$ for firing rate and bursting, respectively) and those measured in WT untreated mice ($P = 0.30$ and $P = 0.48$).

NEUROSCIENCE

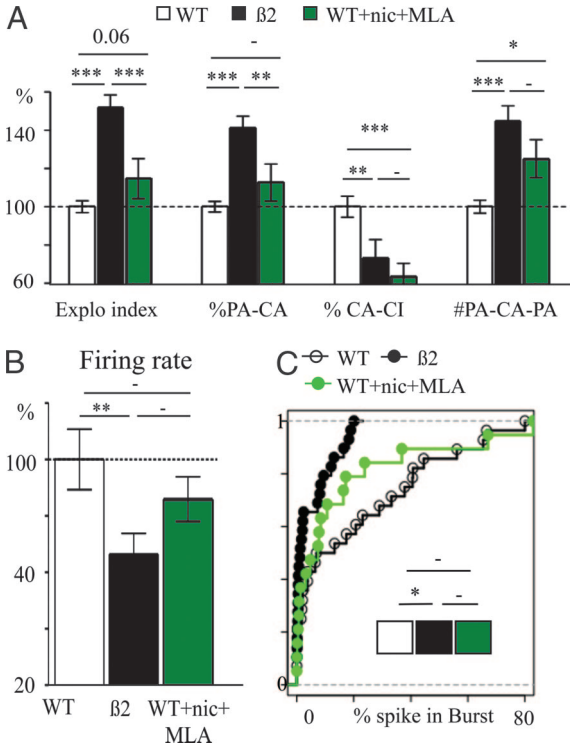

Fig. 4. MLA revealed underlying adaptations in WT. (*A*) Comparison of parameters quantifying exploratory behaviors in saline condition ($n = 29$) and under nicotine or nicotine + MLA exposure ($n = 10$). The value observed in $\beta2^{-/-}$ under saline condition ($n = 15$) is added for comparison. Parameters are normalized by values obtained in WT animals under saline condition (=100%; horizontal dashed line, mean ± SEM). ANOVA indicate statistically significant differences between the three groups $F(2, 51) = 1e\text{-}10$, $2e\text{-}5$, $5e\text{-}4$, and $8.5e\text{-}6$ for the four parameters, respectively. Probability of post hoc comparisons between two means are indicated above corresponding vertical. Detailed analyses in WT under chronic nicotine + MLA indicate that movement implying stop behavior in the center and fast crossing (% CA-CI and #PA-CA-PA) was lost and falls to a level comparable to that observed in $\beta2^{-/-}$ mice. (*B* and *C*) Firing of VTA DA cells in WT under saline condition ($n = 28$ cells) and nicotine + MLA exposure ($n = 31$ neurons) and in $\beta2^{-/-}$ under saline condition ($n = 29$ neurons). (*B*) Barplot of mean frequency of VTA DA neurons (mean ± SEM) normalized to the frequency observed in WT animals (=100%; horizontal dashed line). ANOVA indicate statistically significant differences between the three groups $F(2, 72) = 0.02$. Probability of post hoc comparisons between two means are indicated above corresponding horizontal lines. (*C*) Cumulative distribution of percentage of burst firing. Kruskal–Wallis rank sum test, $P = 0.04$. Probability of post hoc comparisons (Wilcoxon test) between two means are indicated above corresponding horizontal lines (−, $P > 0.05$; *, $P < 0.05$; **, $P < 0.01$; *** $P < 0.001$).

These alterations, revealed by the simultaneous blockade of $\alpha7$*nAChR and exposure of $\beta2$*nAChRs to nicotine, indicate that a latent long-term adaptation had occurred in WT animals with functional $\alpha7$*nAChR and $\beta2$*nAChRs. Such an adaptative mechanism would require both receptor subtypes and would result in apparently normal exploratory behavior and electrophysiological properties of DA neurons.

Discussion

Our present results describe long-term homeostatic processes that occur when WT and genetically or pharmacologically modified mice are chronically exposed to nicotine. We provide evidence that, in WT animals, at the dose we used and in the circumscribed framework of our experiments, chronic nicotine does not produce any explicit behavioral and physiological effects despite profound neurochemical modifications involving both $\beta2$- and $\alpha7$*nAChRs. These effects are unmasked when either the $\beta2$*nAChRs or the $\alpha7$*nAChRs are no longer available.

To account for these observations, we propose as a working hypothesis that chronic nicotine modifies the balance between at least two "opposing" processes, orchestrated by both the $\beta2$*nAChRs and the $\alpha7$*nAChRs. The hypothesis illustrated in Fig. 5 proposes the following.

(*i*) The first "negative" effect of chronic nicotine is to render the $\beta2$*nAChR unavailable through desensitization, in agreement with the classical model proposed by Dani and Heinemann (13). Consistent with this view, WT mice exposed to chronic nicotine show a $\beta2^{-/-}$-like phenotype when the compensatory process triggered by $\alpha7$ is blocked. Data obtained *in vitro* further suggest that low doses of nicotine preferentially desensitize the non-$\alpha7$*nAChRs present on VTA neurons (30) through "high-affinity desensitization" (31). This mechanism plausibly accounts for the observed dissociation between $\beta2$*- and $\alpha7$*nAChRs.

(*ii*) The second effect of chronic nicotine, which may be termed "positive," counteracts the $\beta2$-driven inactivation caused by desensitization through the involvement of $\alpha7$*nAChRs. It is triggered independently of $\beta2$*nAChRs desensitization, because it gives rise to restoration of the impaired function in $\beta2^{-/-}$ mice. The administration of MLA blocks the development of this effect in both WT and $\beta2^{-/-}$ and it thus is mediated via $\alpha7$*nAChRs. Yet, $\alpha7$*nAChRs do not up-regulate. On the other hand, the restoration of the presynaptic cholinergic sites observed under chronic nicotine in $\beta2^{-/-}$ mice leads to the proposal of an enhanced tonic release of endogenous acetylcholine, which remains to be demonstrated. Such enhanced cholinergic transmission would mobilize $\alpha7$*nAChRs located either on the ACh striatal interneurons and/or on the glutamatergic terminals originating from the prefrontal cortex.

As suggested by electrophysiological recordings, the restoration that we observe likely involves mesocorticostriatal dopaminergic pathways, the site of restoration of choline uptake. Moreover, the restored behaviors, previously shown to involve exploration and novelty seeking (see also *SI Text*), were also those specifically altered by a modification of $\beta2$*nAChRs activity within the VTA (8). Our results, however, do not exclude that other behaviors that depend on different neural pathways are modified by chronic exposure to nicotine (32).

The present data obtained with WT and mutant mice are consistent with the proposed hypothesis. On the other hand, several aspects of the addictive process caused by nicotine exposure remain to be understood. A first one is the contribution of high-affinity nAChRs up-regulation, which does not appear clearly in our experiments. Another important concern is the precise location of the observed long-term changes in cholinergic brain circuits. Our previous analysis of the firing pattern of VTA DA cells (11) indeed revealed that endogenous ACh activation of $\beta2$*nAChR gives access to an excitable neuronal state and enhanced bursting patterns. We demonstrate here that this role of $\beta2$*nAChRs can be bypassed by a process that depends on both $\alpha7$*nAChRs activation and chronic nicotine exposure. An interesting possibility would then be that chronic nicotine causes a long-term modification of the presynaptic properties of glutamatergic terminals in VTA, a mechanism that involves $\alpha7$*nAChRs (33). Burst firing has been suggested to be elicited by facilitating the presynaptic release of glutamate and to involve as well $\alpha7$*nAChRs (34). Such long-term modifications might account for the effect of MLA observed in our experiments with chronic nicotine.

However, in $\beta2^{-/-}$ mice, the regional recovery of cholinergic activity, measured by hemicholinium binding, within the striatum that parallels the recovery of electrophysiological parameters in VTA suggests additional locations of the long-term effect and identifies the striatum as a potentially important target.

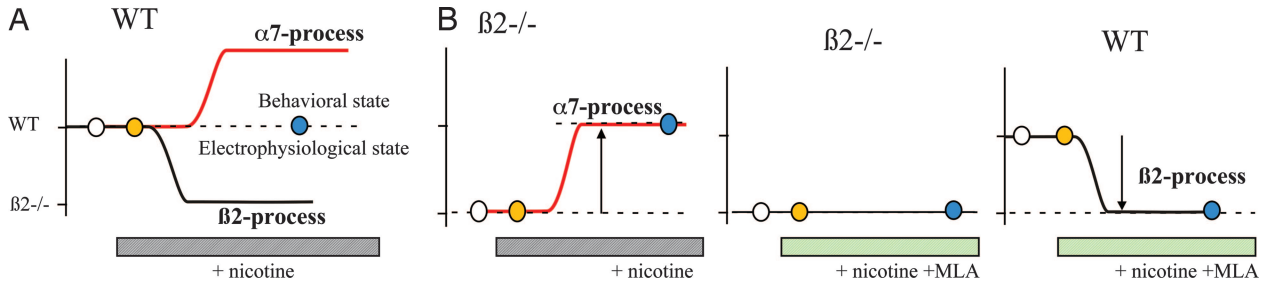

Fig. 5. Proposed process. (*A*) Two opposing processes in nAChRs function adaptation. Chronic exposure to nicotine triggered two processes that add together. Black and red lines indicate the separate processes, called α- and β-process, respectively, that add together to cause the state observed at behavioral and electrophysiological levels. (*B*) Summarized experimental evidence for these two processes. (*Left*) The overall state in $\beta2^{-/-}$ mice is different from that observed in WT. After chronic nicotine exposure, a process that compensates the initial differences is triggered. (*Center*) This process in $\beta2^{-/-}$ mice is blocked by MLA. (*Right*) Adding MLA to nicotine in WT revealed another process. White, yellow, and blue circles represent behavioral and electrophysiological states of the mice before, during 3 days, and during 28 days of chronic exposure, respectively.

In summary, our data obtained in mice provide evidence for a functional balance between nicotinic receptors subtypes that might also take place in smokers under nicotine exposure. The data from mice also suggest a mechanism that may account for the pharmacological effects of nicotine observed under pathological conditions (35) such as Alzheimer's disease, schizophrenia, and autism that have been reported to differentially affect nAChRs subtypes (36). Indeed, the high prevalence of smokers in schizophrenic and ADHD patients suggests that chronic nicotine intake may be a form of self-medication (37) that could reflect action of α7-dependent compensatory mechanism. The present results on the long-term compensatory effects affecting balance between $\beta2$*- vs. $\alpha7$*nAChRs caused by chronic nicotine exposure in mice thus pave the way for the design and development of nicotine-like agents for the treatment of human pathologies. These disease states represent outstanding targets for the chronic actions of novel nicotinic drugs.

Methods

Animals. The construction of the genetically modified mice deleted (KO) for the $\beta2$ nicotinic subunit gene ($\beta2^{-/-}$) has been described in ref. 38. C57BL6/J WT control mice and $\beta2^{-/-}$ mutant siblings (from parents backcrossed for 19 generations to the C57BL6/6J parental strain) were supplied by Charles River Laboratories (L'arbresle, France). Mice were housed individually under a 12-h light-dark cycle in rooms at a controlled temperature (21°C) with free access to water and food. All experiments were carried out during the light phase, between 10 a.m. and 6 p.m. All mice were males aged between 3 and 5 months at the beginning of the experiments. Experiments were carried out following the guidelines of the European Communities Council (86/609/EEC).

Drugs. Nicotine hydrogen tartrate salt (Sigma) and methyllycaconitine citrate (Sigma) were dissolved in sterile saline solution (0.9% NaCl). The pH was adjusted to 7 with NaOH.

Surgical Implantation of Minipumps. Mice were slightly anesthetized with a xylazine and ketamine combination (15% xylazine/2.5% ketamine/82.5% PBS). Osmotic minipumps (model 2004, ALZET; DURECT) were implanted s.c. at the nape of the neck. They delivered nicotine, MLA, nicotine + MLA, or saline solutions at a constant rate (2.4 mg/kg per day for nicotine and 0.24 mg/kg per day for MLA as MLA has a stronger affinity for $\alpha7$*nAchRs for a period of 28 days). All experiments were carried out between the 21st and the 27th day of nicotine delivery, except the control exploratory experiment for which animals were tested 3 days after the beginning of delivery (see *SI Text*).

Exploratory Activity. Exploratory activity was measured in a 1-m-diameter circular open field. Experiments were performed out of the sight of the experimenter and a video camera, connected to a Videotrack system (View-point, Lyon, France), and recorded the trajectories of the mice for 30 min.

The Videotrack system was set up to differentiate the different types of displacements: navigation (speed $\geq$14.4 cm/sec) and exploration (speed $\leq$14.4 cm/sec). The time spent in each type of behavior was automatically measured. Such measures, however, do not describe the alternations and sequences between these complementary locomotor behaviors. Therefore, we adopted a second approach that consisted in a symbol-based analysis of the trajectories (18, 39). The arena (diameter of 1 m) was virtually divided into a central zone (C, 65 cm) and a peripheral zone (P, 35 cm). The instantaneous velocity was divided into two categories: activity (A, $>$ 8.75 cm/sec) and inactivity (I, $<$ 8.75 cm/sec). Then, the symbols were combined to obtain four states: activity in the central zone (CA), inactivity in the central zone (CI), activity in the peripheral zone (PA), and inactivity in the peripheral zone. Overall, four parameters then were defined:

Index. The index of exploration defined as the ratio of the time spent in exploration divided by the time spent in navigation.

%PA-CA. The conditional probability of transition from state PA to state CA, expressed as a percentage. For example, 60% means that given that the mouse was in PA state, the next state will be CA in 60% of the cases.

%CA-CI. The conditional probability of transition from state CA to state CI, also expressed in percentage.

#PA-CA-PA. The total number of large movements across the center of the open field. Expressed as an absolute number, it counts the number of PA-CA-PA sequences.

***In Vivo* Electrophysiology: Extracellular Single-Cell Recordings.** As described in detail in previous publications (11), anesthetized mice were equipped with recording electrodes within the VTA and DA neurons were distinguished from non-DA neurons by their electrophysiological properties (26, 40). DA cell firing *in vivo* was analyzed with respect to the average firing rate and the percentage of spikes within a burst (number of spikes within burst divided by total number of spikes). Bursts were identified as discrete events consisting of a sequence of spikes such that (*i*) their onset are defined by two consecutive spikes within an interval lower than 80 msec, whenever (*ii*) they terminated with an interval of $>$160 msec.

Receptor Autoradiography. Coronal sections (20 μm) were incubated at room temperature with 200 pM [^{125}I]-epibatidine (PerkinElmer, Boston, MA; specific activity 2,200 Ci/mmole; 1

NEUROSCIENCE

Ci = 37 GBq) in 50 mM Tris (pH 7.4) for 30 min. After incubation, sections were rinsed twice for 5 min each in the same buffer and briefly in distilled water. Sections then were exposed to Kodak Biomax films overnight. For [^{3}H]Hemicholinium-3 binding, 20-μm sections were incubated with 8 nM [^{3}H]Hemicholinium-3 (PerkinElmer; specific activity 125 Ci/mmole) at 4°C for 60 min in 50 mM Tris (pH 7.4) containing 300 mM NaCl. After incubation, sections were rinsed six times for 1 min each in ice-cold 50 mM Tris (pH 7.4) and briefly in distilled water. Nonspecific binding was measured in the presence of 100 μM nonlabeled hemicholinium-3. Sections then were exposed for 21 days to Kodak Biomax films. Densitometric analysis in specific brain regions was performed for each radioactive ligand by using Image J software (NIH Image) and appropriate standards. For reference, SI Fig. 6 sections can be compared with figures 28, 46, and 56 (top to bottom) from the mouse atlas of Paxinos and Franklin (41).

Statistical Analysis. All data were analyzed by using StatView version 5.0 and R, a language and environment for statistical computing. Data are plotted as mean ± SEM. Boxplot was used for %SWB, because the distribution of this parameter does not conform to normal one. Total number (n) of observations in each group and statistic used are indicated in figure legend.

Autoradiographic data (Fig. 1) were analyzed by using the two samples Wilcoxon tests also known as Mann–Whitney test.

Data concerning exploratory activity were analyzed by using the Student t test (Fig. 1) or one-way ANOVAs and the Fisher post hoc test (Figs. 2 and 4). df designated the degrees of freedom for the statistic.

Electrophysiological data: Distribution of the mean firing rate conforms to a normal distribution, whereas distribution of %SWB does not. Mean firing then was analyzed by using the Student t test (Fig. 1) or one-way ANOVAs and the Fisher post hoc test (Figs. 2 and 4), whereas %SWB was analyzed by using the Wilcoxon test (Fig. 1) or Kruskal–Wallis rank sum test of the null hypothesis that the location parameters of the distribution of %SWB are the same in each of the four groups. If significant, this test was followed by the Wilcoxon test between groups (Figs. 2 and 4).

[^{3}H]-Hemicholinium-3 binding (Fig. 3) was analyzed by using two-way ANOVA. Upon significant effects in one source of variation ("genotype," "treatment," or interaction between factors), data were analyzed further by using the Fisher post hoc test.

We thank Trevor Robbins, Boris Gutkin, and Patrick Love for comments on the manuscript. This research was supported by the Institut Pasteur, Collège de France, Centre National de la Recherche Scientifique (CNRS) Unité de Recherche Associée 2182 and Unité Mixte de Recherche 5106, l'Agence National de la Recherche (ANR), Association de Recherche sur le Cancer, the Letten F. Saugstad Foundation (M.B.), the Fondation pour la Recherche Médicale (M.B.), and the Fondation Gilbert Lagrue pour la Recherche sur la Dépendance Tabagique (N.M.).

1. Changeux JP, Edelstein SJ (2005) *Nicotinic Acetylcholine Receptors: From Molecular Biology to Cognition* (Odile Jacob, New York).
2. Grenhoff J, Aston-Jones G, Svensson TH (1986) *Acta Physiol Scand* 128:351–358.
3. Pontieri FE, Colangelo V, La Riccia M, Pozzilli C, Passarelli F, Orzi F (1994) *NeuroReport* 5:2561–2564.
4. Picciotto MR (2003) *Trends Pharmacol Sci* 24:493–499.
5. Corrigall WA, Coen KM, Adamson KL (1994) *Brain Res* 653:278–284.
6. David V, Besson M, Changeux JP, Granon S, Cazala P (2006) *Neuropharmacology* 50:1030–1040.
7. Besson M, David V, Suarez S, Cormier A, Cazala P, Changeux JP, Granon S (2006) *Psychopharmacology* 187:189–199.
8. Maskos U, Molles BE, Pons S, Besson M, Guiard BP, Guilloux JP, Evrard A, Cazala P, Cormier A, Mameli-Engvall M, *et al.* (2005) *Nature* 436:103–107.
9. Picciotto MR, Zoli M, Rimondini R, Lena C, Marubio LM, Pich EM, Fuxe K, Changeux JP (1998) *Nature* 391:173–177.
10. Laviolette SR, van der Kooy D (2004) *Nat Rev Neurosci* 5:55–65.
11. Mameli-Engvall M, Evrad A, Pons S, Maskos U, Svensson TH, Changeux JP, Faure P (2006) *Neuron* 50:911–921.
12. Rahman S, Zhang J, Engleman EA, Corrigall WA (2004) *Neuroscience* 129:415–424.
13. Dani JA, Heinemann S (1996) *Neuron* 16:905–908.
14. Pidoplichko VI, DeBiasi M, Williams JT, Dani JA (1997) *Nature* 390:401–404.
15. Staley JK, Krishnan-Sarin S, Cosgrove KP, Krantzler E, Frohlich E, Perry E, Dubin JA, Estok K, Brenner E, Baldwin RM, *et al.* (2006) *J Neurosci* 26:8707–8714.
16. McCallum SE, Collins AC, Paylor R, Marks MJ (2006) *Psychopharmacology* 184:314–327.
17. Serova L, Sabban EL (2002) *J Pharmacol Exp Ther* 303:896–903.
18. Granon S, Faure P, Changeux JP (2003) *Proc Natl Acad Sci USA* 100:9596–9601.
19. Grabus SD, Martin BR, Batman AM, Tyndale RF, Sellers E, Damaj MI (2005) *Psychopharmacology* 178:183–192.
20. Nomikos GG, Hildebrand BE, Panagis G, Svensson TH (1999) *NeuroReport* 10:697–702.
21. Matta SG, Balfour DJ, Benowitz NL, Boyd RT, Buccafusco JJ, Caggiula AR, Craig CR, Collins AC, Damaj MI, Donny EC, *et al.* (2007) *Psychopharmacology* 190:269–319.
22. Buisson B, Bertrand D (2002) *Trends Pharmacol Sci* 23:130–136.
23. Flores CM, Rogers SW, Pabreza LA, Wolfe BB, Kellar KJ (1992) *Mol Pharmacol* 41:31–37.
24. Parker SL, Fu Y, McAllen K, Luo J, McIntosh JM, Lindstrom JM, Sharp BM (2004) *Mol Pharmacol* 65:611–622.
25. Mansvelder HD, Keath JR, McGehee DS (2002) *Neuron* 33:905–919.
26. Grace AA, Bunney BS (1983) *Neuroscience* 10:317–331.
27. Salas R, Pieri F, De Biasi M (2004) *J Neurosci* 24:10035–10039.
28. Ribeiro FM, Black SA, Prado VF, Rylett RJ, Ferguson SS, Prado MA (2006) *J Neurochem* 97:1–12.
29. Beeri R, Le Novere N, Mervis R, Huberman T, Grauer E, Changeux JP, Soreq H (1997) *J Neurochem* 69:2441–2451.
30. Wooltorton JR, Pidoplichko VI, Broide RS, Dani JA (2003) *J Neurosci* 23:3176–3185.
31. Giniatullin R, Nistri A, Yakel JL (2005) *Trends Neurosci* 28:371–378.
32. Cohen G, Roux JC, Grailhe R, Malcolm G, Changeux JP, Lagercrantz H (2005) *Proc Natl Acad Sci USA* 102:3817–3821.
33. Mansvelder HD, McGehee DS (2000) *Neuron* 27:349–357.
34. McGehee DS, Heath MJ, Gelber S, Devay P, Role LW (1995) *Science* 269:1692–1696.
35. Newhouse P, Singh A, Potter A (2004) *Curr Top Med Chem* 4:267–282.
36. Cassels BK, Bermudez I, Dajas F, Abin-Carriquiry JA, Wonnacott S (2005) *Drug Discov Today* 10:1657–1665.
37. Sacco KA, Bannon KL, George TP (2004) *J Psychopharmacol* 18:457–474.
38. Picciotto MR, Zoli M, Lena C, Bessis A, Lallemand Y, Le Novere N, Vincent P, Pich EM, Brulet P, Changeux JP (1995) *Nature* 374:65–67.
39. Faure P, Neumeister, H., Faber D, Korn H (2003) *Fractals* 11:233–243.
40. Grace AA, Bunney BS (1984) *J Neurosci* 4:2877–2890.
41. Paxinos G, Franklin KBJ (2004) *The Mouse Brain in Stereotaxic Coordinates* (Elsevier, San Diego).